

Effect of pressure on the electronic structure of ferromagnetic nickel and iron

L. I. Vinokurova, A. G. Gapotchenko, E. S. Itskevich, É. T. Kulatov, and N. I. Kulikov

Institute of High Energy Physics, USSR Academy of Sciences
 (Submitted 26 October 1978)
 Zh. Eksp. Teor. Fiz. 76, 1644–1654 (May 1979)

Measurements of the frequencies of the de Haas–van Alphen effect under pressure show, for iron and nickel, an anomalously large difference between the baric coefficients of the extremal Fermi-surface sections. To explain this effect, the band structure and the Fermi surfaces are calculated by using the model-Hamiltonian method (approximate method of solving the secular equation of the Korringa–Kohn–Rostoker theory). It is shown that different contributions, such as the spillover of electrons from one spin subsystem to the other and the change of the crystal potential under pressure, have different pressure dependences and determine the difference between the baric coefficients.

PACS numbers: 71.25.Hc, 71.25.Pi

1. INTRODUCTION

It is now more or less universally accepted that ferromagnetism and antiferromagnetism of transition metals can be explained within the framework of the band model, i.e., of the single-electron approximation, in which exchange–correlation effects are taken into account with the aid of the statistical X_α method developed by Slater.¹ In the band theory of ferromagnetism (the Stoner theory) it is assumed that the energy bands are split by the exchange interaction into two subbands, one containing spin-up electrons, which is the band with large number of electrons or the spin subband of the majority electrons, and the other (spin-down) is the spin subband of the minority electrons. Thus, the spontaneous magnetic moment is due to unequal numbers of electrons that fill the spin-polarized energy subband.

In the rigid band model, these subbands are assumed shifted by an amount equal to the exchange splitting energy Δ , but having the same geometry. In a more realistic model the energy splitting depends on the wave vectors, and correspondingly the subbands with spin up (\uparrow) and with spin down (\downarrow) have somewhat different dispersion laws (see Fig. 2 below). However, even in the rigid band approximation, owing to the change in the position of the Fermi level ϵ_F relative to the bottom of the band, the spin-up and spin-down electrons will have different Fermi-surface topologies. Thus, in nickel the Fermi surface of the band with the larger number of electrons is similar with respect to some essential singularities to the Fermi surface of copper, while the Fermi surface of the band with the smaller number of electrons is similar to the Fermi surface of iridium or palladium (see Fig. 1).

Through measurements of the de Haas–van Alphen (dHvA) effect and through theoretical calculations of the band structure, the shapes of the Fermi surfaces of ferromagnetic metals, particularly iron and nickel, have been sufficiently well investigated, and on the whole the experiment confirms Stoner's theory. A survey of the experimental research on the Fermi surfaces of these metals at normal pressure can be found in Ref. 2. The present paper is devoted to a theoretical and ex-

perimental investigation of the change of the Fermi surface with changing volume for one atom, i.e., under the influence of pressure. An earlier review of the results of similar experiments³ is a good introduction to this problem.

Some preliminary results of the investigation of the Fermi surface under pressure for iron and nickel were published in Refs. 4 and 5. The experimental methods are briefly described in these papers and we shall not dwell on them here. It is of interest to note that whereas both the baric coefficients (BC) of the magnetizations of iron and nickel (-3.1×10^{-4} and -2.9×10^{-4} kbar⁻¹ respectively)⁶ and the compressibilities (-5.2×10^{-4} and -5.5×10^{-4} kbar⁻¹) are close, the BC for the measured sections of the Fermi surfaces differ by more than one order of magnitude (see Table I). It is natural to assume that this difference is due to specific features of the band structures of these metals and to the character of their changes under pressure. Principal attention will therefore be paid to a comparison of the experimentally observable quantities and the results of calculations performed "from first principles." We chose for this calculation the method of solving the secular equation of the theory of Korringa, Kohn, and Rostoker (KCR) for a transition metal (model Hamiltonian), proposed by Heine⁸ and developed by Hubbard⁹ and one of us.¹⁰ Some results of a calculation of the pressure-induced change of the Fermi surface of chromium by this method were published in Ref. 11.

The model Hamiltonian of a transition metal has the following structure:

$$(H - ES)X = 0,$$

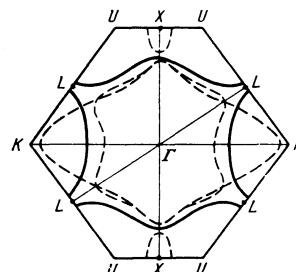


FIG. 1. Section of the Fermi surface of fcc ferromagnetic nickel by the (110) plane. Solid lines—Fermi-surface sections for the more filled band, dashed—for the less filled bands.

TABLE I. Experimental values of baric coefficients of some parts of the Fermi surfaces of nickel and iron

| Section | Orientation | $d \ln S / d \ln V$ | |
|-------------------------------|-------------|--------------------------------|-----------------------|
| | | Present authors ^{4,5} | Anderson ⁷ |
| Nickel | | | |
| Neck \uparrow (L_2') | [111] | -1.5±0.2 | -1.1±0.2 |
| » | [112] | -1.2±0.4 | - |
| Pocket \downarrow (X_5) | [111] | -1.2±0.4 | - |
| » | [112] | -0.3±0.15 | - |
| » | [100] | +0.15±0.15 | -0.2±0.05 |
| Iron | | | |
| Lens \downarrow | [100] | -16.3±4 | - |
| » | [111] | -16±1 | - |
| » | [110] | -17.3±2 | - |

where

$$H = \begin{vmatrix} v & \hbar \\ \hbar^* & t \end{vmatrix}, \quad S = \begin{vmatrix} \delta_{ss'} + \delta_{ss'} & 0 \\ 0 & \gamma^{-1} \delta_{mm'} \end{vmatrix}.$$

The upper diagonal block of the matrix H

$$v = (|k+g|^2 - E) \delta_{ss'} + C_{ss'} - \sum_{\sigma} \frac{V_{g\sigma} V_{g'\sigma}}{\epsilon_{\sigma} - \epsilon_F}$$

describes the potential scattering, the lower diagonal block

$$t = \left(\frac{\epsilon}{\gamma} - E \right) \delta_{mm'} - \sum_{\sigma} \frac{\hbar_{\sigma 2m} \hbar_{\sigma 2m'}}{\epsilon_{\sigma} - \epsilon_F}$$

describes the resonant scattering, and the off-diagonal blocks

$$\hbar = \hbar_{2m\sigma} - \sum_{\sigma'} \frac{V_{g\sigma} \hbar_{\sigma 2m\sigma'}}{\epsilon_{\sigma} - \epsilon_F}, \quad \hbar^* = \hbar_{g2m} - \sum_{\sigma'} \frac{V_{g\sigma'} \hbar_{\sigma 2m}}{\epsilon_{\sigma'} - \epsilon_F}$$

correspond to hybridization.

Here $\epsilon_g = |k+g|^2$;

$$V_{ss'} = \frac{4\pi}{\Omega} \sum_l (2l+1) \gamma_l'(E) j_l(|k+g|r_s) j_l(|k+g'|r_s) P_l(\cos \theta_{ss'})$$

is the matrix element of the potential-scattering block of the KCR method, where γ_l' is the potential-scattering amplitude factor approximated by a function of the energy, i.e., $V_{ss'} = C_{ss'} + ES_{ss'}$; the quantity

$$\hbar_{g2m} = 4\pi \Omega^{-1/2} j_l(|k+g|r_s) Y_{l-2, m}(\mathbf{k}+g)$$

is the hybridization matrix element, $Y_{lm}(\mathbf{x})$ is a cubic harmonic that depends only on the direction of the vector \mathbf{x} , i.e., on $\mathbf{x}/|\mathbf{x}|$; $j_l(x)$ is a spherical Bessel function, $P_l(x)$ is a Legendre polynomial, l and m are the orbital and magnetic quantum numbers, Ω is the volume of the unit cell, and g is the reciprocal-lattice vector included in the basis of the model Hamiltonian (usually the vectors from the first coordination sphere and some vectors from the second), and G are the reciprocal-lattice vectors, scattering from which is taken into account in second-order perturbation. A more detailed description of the method of the model Hamiltonian of the KCR method can be found in Refs. 10 and 12.

Thus, the crystal muffin-tin (MT) potential is characterized by only eight parameters, namely, the parameters of the expansion of the function $\gamma_l'(E, r_s) = a_l + b_l E$ for $l=0, 1, 2$ (r_s is the radius of the sphere of the MT potential) and the resonant-scattering parameters

ϵ and γ . Only these eight numbers are needed to describe the band structure of any particular transition metal.

2. FERMI SURFACE AND BAND STRUCTURE OF NICKEL AND ITS CHANGE UNDER PRESSURE

The Fermi surface of fcc nickel obtained in a number of experimentals (e.g., Ref. 13) and theoretical^{14, 15} studies as cut by the (110) plane is shown in Fig. 1. Using the dHvA procedure in a chamber with fixed pressure, we measured the section of the neck near the L point of the majority spin subband and of the pocket near the X point for the minority spin subband.⁴ The pressure dependences of these sections obtained in our measurements⁴ and by Anderson⁷ are shown in Table I. It is seen that for the neck L_2' the results of both experiments agree within the limits of error, but even very small baric coefficients (BC) for the X_5 pocket in the (100) plane have opposite signs.

If the decrease of the magnetization of the ferromagnet with increasing pressure is treated within the framework of the Stoner theory, this means that the exchange splitting Δ decreases, the subbands with different spins come closer together, a redistribution of the electrons in the spin bands takes place, and the volumes of the parts of the Fermi surface change. If it is assumed that this is not accompanied by a change in the effective mass, ($d \ln m^* / d p = 0$), then we can obtain a formula for the BC of the section within the framework of the Fermi surface of the hard band⁵ and express the change of the section in terms of the change of the magnetization:

$$\frac{d \ln S}{d \ln V} = B_M = \pm \frac{m^* \Delta}{e \hbar F} \left(\frac{N_{\sigma}}{N_{\uparrow} + N_{\downarrow}} \right) \frac{d \ln M}{d \ln V} \quad (1)$$

(the plus and minus signs are for $\sigma = \uparrow$ and $\sigma = \downarrow$). Here $d \ln M / d \ln V = d \ln \Delta / d \ln V = +0.53$ for nickel according to the data of Kondorskii and Sedov,⁶ Δ is the exchange splitting, F is the frequency of the oscillations of this section, N is the state density, and M is the magnetization. For the neck L_2' we obtain from (1) $B_M = +1.3$, which disagrees with the results of both direct experiments (see Table I). This qualitative difference between the experimental data and the results of a calculation by a simple model can be due to the presence of other contributions to the change of the cross section.

To separate contributions of different character to the change of the Fermi surface under pressure, we compare the properties of the spectrum of a ferromagnetic metal with a nonferromagnetic one (which we shall call a model one), having the same crystal structure having near ϵ_F an electron spectrum similar to one of the spin subbands, and having a compressibility $d \ln V / d p$, as close as possible to the compressibility of our ferromagnet. It follows from the experimental data that for nonferromagnetic metals possessing this similarity, the BC of the corresponding sections have the same sign and are close in value. For the model metal, the change of the Fermi surface is due only to the change of the potential due to the change of the interatomic distance, and by the scale effect due to the change in the dimensions of the Brillouin zone (potential contribution to BC).

For a ferromagnet there is added to the fundamentally important effect of the change of the Fermi surface because of the redistribution of the electrons among the spin subbands under pressure (the magnetic contribution to the BC). Using the proximity of the values of the BC for metals that enter in similar groups, we can assume, for qualitative estimates, that the potential component of the BC of a ferromagnetic metal is equal to the BC of the model metal. For the majority spin subband in nickel this model metal is copper. To take into account the difference between the compressibilities of the metals, it is necessary to add to the magnetic contribution to the BC not the values of $d \ln S / dp$, which are usually cited as the result of the experiments, but

$$\frac{d \ln S}{d \ln V} = \frac{d \ln S}{dp} / \frac{d \ln V}{dp}.$$

The assumption that the resultant BC of the ferromagnet is a sum of a potential and a magnetic contribution provides a good estimate for the BC of the section of the neck L'_2 in nickel at $\mathbf{H} \parallel [111]$:

$$\frac{d \ln S}{d \ln V} = B_M + \left(\frac{d \ln S}{d \ln V} \right)_{cu} = 1.3 - 2.5 = -1.2, \quad (2)$$

which is in satisfactory agreement with the results presented in Table I. Getting ahead of ourselves, we indicate that this model gives good agreement with our measurements of the BC of the sections of the lens of the Fermi surface of iron if the model metal is taken to be molybdenum.

It is necessary, however, to compare these results with the data obtained without using empirical considerations. To this end we have calculated the band structure of ferromagnetic nickel, using a spin-dependent potential to determine the parameters of the model Hamiltonian.

We calculated first the paramagnetic potential of nickel by superimposing the self-consistent atomic potentials of Herman and Skillman¹⁶ by the method proposed by Mattheiss.¹⁷ The exchange interaction was introduced via the Slater statistical exchange potential

$$V_{ex} = -6[3\rho(r)/8\pi]^{1/2},$$

[$\rho(r)$ is the electron density in the crystal]. Assuming that the polarization is produced only by d electrons, we can obtain for an electron density with different spins

$$2\rho = \rho_{para} \pm \frac{n_\sigma}{n_d} \rho_d(r), \quad (3)$$

where n_σ is the number of electrons per atom in the spin subbands, n_d is the total number of the d electrons, and ρ_d is the density of the d electrons in the crystal. The spin-dependent potential is then obtained by substituting (3) in V_{ex} .

We obtained the band structures of nickel for the normal lattice constant $a = 6.65$ a.u. and for the constant decreased 3%, corresponding to a pressure of 164 kbar. This relatively high pressure was necessitated by the calculation accuracy, which was not sufficient at pressures ~ 10 kbar. At normal pressure, the Fermi surface of nickel agrees with calculation by others and coincides with Fig. 1.

From the calculation of the state density we determined the Fermi energy at normal and high pressure. The value of ϵ_F at normal pressure, 0.66 Ry, was corrected by +0.004 Ry, after which we obtained the dimensions of the principal semiaxes of the ellipsoidal pocket X_5 (in units of $2\pi/a$): $XW = 0.1(0.098)$, $XU = 0.112(0.112)$, $\Gamma X = 0.208(0.196)$, and the neck radius: $LW = 0.051(0.048)$. In the parentheses are given the experimental values. No fundamental changes occur under pressure. For the BC of the change of the intersection of the pocket with the (100) plane and the intersection of the neck with the (111) plane our calculation yields respectively

$$d \ln S_{(100)} / d \ln V = 1.1, \quad d \ln S_{(111)} / d \ln V = -1.8.$$

The result for the section L'_2 agrees qualitatively with the estimate obtained with the aid of the model metal [see(2)] and is close to the experiment.

The substantial quantitative difference in the case of the BC of the X_5 pocket may be due to two causes: First, to the non-self-consistency of the potential constructed by the Mattheiss method, and second, to the complexity of localization of the position of the Fermi energy in calculations made from first principles, whose accuracy does not exceed 0.005 Ry. A fit of the position of the Fermi level within the limits of this error yields the experimentally measured values of the BC, but this procedure, which is sometimes used, does not add in our opinion to the reliability of the results. We have therefore carried out an additional calculation of the band structure of the ferromagnetic nickel, using self-consistent potentials obtained for the spin subbands by Wakoh,¹⁴ who used the KCR method. The exchange interaction was introduced for these potential by a method in fact analogous to that described above. The model-Hamiltonian parameters for the non-self-consistent potential at normal pressure and at 164 kbar, and also the parameters that approximate the Wakoh potential, are given in Table II.

The band structure in the principal high-symmetry directions for both spin subbands, obtained by the model Hamiltonian with a Wakoh potential, is shown in Fig. 2 and agrees well with Wakoh's calculations.¹⁴ Thus, the gaps are $X_5^{\uparrow} - X_5^{\downarrow} = 0.073$ (0.074), $X_2^{\uparrow} - X_2^{\downarrow} = 0.072$ (0.073), $L_2^{\uparrow} - L_2^{\downarrow} = 0.015$ (0.016), and $\Gamma_1^{\uparrow} - \Gamma_1^{\downarrow} = 0.017$ (0.018). The values of the gaps are in Rydbergs, and the quantities in the parentheses are those calculated by Wakoh.¹⁴ We note that if we accept Krinchik's interpretation¹⁹ and change the sequence of the levels at the point L for the majority spin subband, then the gap is $L_2^{\downarrow} - L_2^{\uparrow} = 0.056$ Ry.

The energies in 91 points of 1/48 of the irreducible part of the Brillouin zone of an fcc lattice were used to calculate the state density and to determine the position of the Fermi energy. The value of ϵ_F obtained by us at $n_1 = 5.33$ agrees with that given by Wakoh¹⁴: $\epsilon_F^{\uparrow} = 0.742$ Ry. The state densities at $p = 0$ are $N_1(\epsilon_F) = 22.3 \text{ Ry}^{-1} \times \text{atom}^{-1}$, $N_1(\epsilon_F) = 2.8 \text{ Ry}^{-1} \times \text{atom}^{-1}$. Hence $N_1 / (N_1 + N_2) = 0.11$ and $N_1 / (N_1 + N_2) = 0.89$, which are close to the values 0.1 and 0.9 obtained in Ref. 15. The exchange splitting Δ between the subbands, on the basis of a calcula-

TABLE II. Model-Hamiltonian parameters that characterize the potential

| Parameter* | Nickel | | | | | | Iron | |
|--------------|---------------------|---------|------------|---------|-------------------------------|--------|--|---------|
| | Mattheiss potential | | | | Wakoh potential ¹⁴ | | Potential of Wakoh and Jamashita ¹⁸ | |
| | p=0 | | p=164 kbar | | p=0 | | p=0 | |
| | Spin↑ | Spin↓ | Spin↑ | Spin↓ | Spin↑ | Spin↓ | Spin↑ | Spin↓ |
| r_1 , a.e. | 2.3396 | 2.3396 | 2.2255 | 2.2255 | 2.3511 | 2.3511 | 2.3383 | 2.3383 |
| A_0 | 0.01181 | 0.0123 | 0.0599 | 0.0600 | 0.0210 | 0.0331 | 0.0500 | 0.07615 |
| B_0 | 0.3434 | 0.3440 | 0.3385 | 0.3385 | 0.3197 | 0.3310 | 0.3379 | 0.3572 |
| A_1 | -0.0246 | -0.0236 | 0.0606 | 0.0607 | -0.0031 | 0.0229 | 0.1045 | 0.1653 |
| B_1 | 0.0373 | 0.0380 | 0.0700 | 0.0701 | 0.0853 | 0.1043 | 0.1287 | 0.1588 |
| A_2 | 0.1768 | 0.1778 | 0.2059 | -0.2060 | 0.2107 | 0.2416 | 0.1922 | 0.1519 |
| B_2 | 0.6734 | 0.0740 | 0.0757 | 0.0758 | 0.0889 | 0.0982 | 0.0736 | 0.1088 |
| ϵ | 0.7386 | 0.7332 | 0.8636 | 0.8641 | 0.7430 | 0.8173 | 0.7550 | 0.8995 |
| γ | 1.6913 | 1.6950 | 1.9799 | 1.9803 | 1.8353 | 1.8827 | 2.3606 | 2.4552 |

*The coefficients here are $A_l = 4\pi(2l+1)a_l/\Omega$ and $B_l = 4\pi(2l+1)b_l/\Omega$.

tion of the state density, is 0.07 Ry, which also agrees with the earlier calculations.

If we use the information on the change of the exchange splitting under pressure from the experimental results of Kondorskii and Sedov⁶ and our calculated data on the state density, then we can determine from Stoner's theory the change of the Fermi energy:

$$\frac{d\epsilon_F^\uparrow}{dp} = -\frac{N_\uparrow}{N_\uparrow+N_\downarrow} \frac{d\Delta}{dp} \quad \frac{d\epsilon_F^\downarrow}{dp} = \frac{N_\downarrow}{N_\uparrow+N_\downarrow} \frac{d\Delta}{dp} \quad (4)$$

In compressed nickel (164 kbar) we then have $\delta\epsilon_F^\uparrow = -0.003$ Ry and $\delta\epsilon_F^\downarrow = 0.0005$ Ry. At normal pressure the intersection of the plane (001) and the X_3 pocket is $7.1 \times 10^{-2} \text{ \AA}^{-2}$, and in the compressed state calculation using the band structure shown in Fig. 2 and of the results obtained with the aid of formula (5) gives $S = 6.8 \times 10^{-2} \text{ \AA}^{-2}$. Thus the BC due only to the decrease of the exchange splitting turns out to be equal to $B_M(X_3) = 0.43$. On the other hand if we use as the model metal for the minority spin subband palladium, which has a BC equal to -0.2 (Ref. 20), then the total BC of such a calculation is $\approx +0.2$, which agrees satisfactorily with the experimental data (Table I).

Similar calculations for the neck of the Fermi surface in the majority spin subband yield a value that agrees with the estimate obtained by us previously by using Eq. (1).

Thus, a non-self-consistent but direct calculation, as

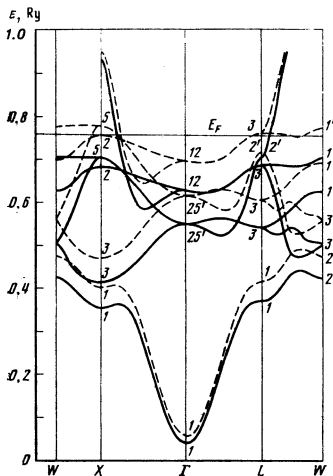


FIG. 2. Band structure of nickel in high-symmetry directions at normal pressure. Solid lines—spin subband of majority electrons, dashed—of minority electrons.

well as the rigid-band approximation for a self-consistent potential, yield for the X_5 pocket a BC smaller by almost one order of magnitude than for the neck, i.e., these calculations confirm both our experimental results and Anderson's results.⁷ There exists, however, a probability that the self-consistent calculation, under pressure, will yield a more appreciable rise of the X_5 level because of the broadening of the band than the increase of the Fermi energy as a result of the cross flow of electrons. In this situation the pocket X_5 can have also a negative BC. A final answer to this question can be obtained only by self-consistency of the crystal potential under pressure, but the physical reason for the smallness of the BC is clear even now: The change of the potential under pressure and the change of the exchange contribution make contributions close in magnitude and opposite in sign.

3. BAND STRUCTURE AND CHANGE OF THE FERMI SURFACE OF IRON UNDER PRESSURE

We have measured the effect of a pressure up to 11 kbar on the section of the so-called lens in the minority spin subband of ferromagnetic iron. The section of the Fermi surface of this subband, analogous to molybdenum and paramagnetic chromium, in the Brillouin band of a bcc lattice is shown in Fig. 3. According to the data of Ref. 21, the lens is almost a sphere separated by the spin-orbit interaction from the neck of the neck. Figure 3 shows a Fermi surface calculated without allowance for the spin-orbit interaction. We shall neglect this effect in all the calculations of the present paper.

The measurements in the experiment were made in magnetic fields oriented along the crystal axes [100], [110], and [111]. The obtained BC are given in the lower part of Table I.

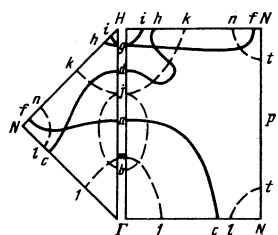


FIG. 3. Section of Fermi surface of iron. Solid and dashed lines—spin subbands of majority and minority electrons.

If we use Eq. (1), then from the experimental values of the BC of the Fermi-surface sections we can obtain the BC of the change of the spontaneous magnetization, and vice versa. If we subtract from the experimental BC of iron, by way of a correction, the BC of the model metal (molybdenum, whose Fermi surface is unusually similar to the Fermi surface of iron), which is equal to -3.9 , then the part of the BC connected with the magnetic percolation is equal to -12 . The resultant value $d \ln M / d \ln V = +0.61$ agrees well with the directly measured $+0.59$.⁶

Iron has a bcc crystal structure with a lattice constant $a = 5.40$ a.u. at helium temperatures. Calculation of the band structure of the iron was made in 55 points of $1/48$ of the irreducible part of the Brillouin zone, with the model-Hamiltonian parameters obtained with the aid of the self-consistent crystal potential of Wakoh and Jamashita.¹⁸ The model-Hamiltonian parameters approximating this potential are also listed in Table II. Histograms of the state densities were constructed for each of the spin subsystems. The calculated band structure in the high-symmetry directions is shown in Fig. 4. The Fermi energy $\epsilon_F = 0.0543$ Ry for both subbands was determined from the condition that the majority and minority subbands contain 5.1 and -2.9 electrons, respectively.

In Table III are given some extremal Fermi-surface sections obtained in the present calculation ($\epsilon_F = 0.654$), in comparison with the results of Wakoh and Jamashita¹⁸ ($\epsilon_F = 0.657$). We note that our calculation gives a more spherical lens than Ref. 18, although the spin-orbit interaction was neglected in both calculations. This interaction, without changing the circular section in the $[100]$ direction, increases the elliptic section.

The exchange-splitting values obtained from the band calculations agree well with the results of Wakoh and Jamashita:

$$\begin{aligned} \Gamma_1^+ - \Gamma_1^- &= 0.039 \text{ Ry (s-type)} \\ N_1^+ - N_1^- &= 0.033 \text{ Ry (p-type)} \\ \Gamma_{12}^+ - \Gamma_{12}^- &= 0.100 \text{ Ry} \\ H_{23}^+ - H_{23}^- &= 0.139 \text{ Ry (d-type)} \end{aligned}$$

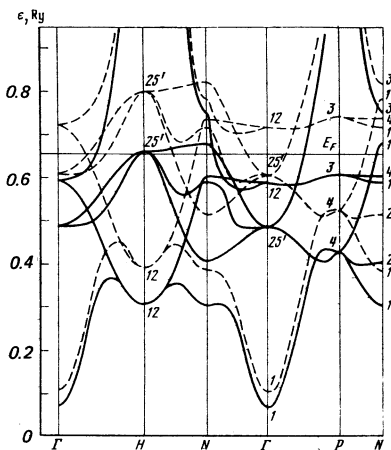


FIG. 4. Band structure of iron at normal pressure. Solid lines—spin subband of majority electrons, dashed—minority electrons.

TABLE III. Comparison of the results of our calculation and that of Wakoh-Jamashita¹⁸ for individual sections of the Fermi surface of iron.

| Extremal section | $S, 10^{-2} \text{ \AA}^{-2}$ | |
|--------------------------------|-------------------------------|--------------------------|
| | MH method* | KCR method ¹⁸ |
| Minority spin subband | | |
| Lens | | |
| elliptic $[100]$ | 1.9 | 2.1 |
| circular $[100]$ | 3.8 | 5.0 |
| Ellipsoid N | | |
| in direction of $H-N$ | 31.4 | 31.3 |
| " $\Gamma-N$ | 44.0 | 47.2 |
| " $\Gamma-N$ | 23.8 | 31.3 |
| Octahedron H : | | |
| in direction of $[100]$ | 161.2 | 215.5 |
| " $[110]$ | 161.3 | 161.6 |
| Sphere | | |
| in direction of $\Gamma-H$ | 19.3 | 26.7 |
| Majority spin subband | | |
| $s-d$ electron surface | | |
| in direction of $[100]$ | 372.0 | 380.0 |
| " $[110]$ | 347.3 | 329.7 |
| Hole pocket H | | |
| in direction of $[100]$ | 4.8 | 4.1 |
| " $[110]$ | 4.2 | 3.6 |
| Hole sleeve in N | 11.2 | 8.7 |
| Maximum section of hole sleeve | 34.5 | 23.2 |

*Model-Hamiltonian method, present paper.

The exchange splitting obtained from the calculation of the state densities in the spin subbands is 0.13 Ry, as against the 0.15 Ry calculated in Ref. 21.

The state densities on the Fermi level at normal pressure were

$$N_+(\epsilon_F) = 7.0 \text{ Ry}^{-1} \cdot \text{atom}^{-1}, \quad N_-(\epsilon_F) = 2.2 \text{ Ry}^{-1} \cdot \text{atom}^{-1}.$$

Thus,

$$N_+ / (N_+ + N_-) = 0.76, \quad N_- / (N_+ + N_-) = 0.24.$$

We note that in the case of iron the ratio of the state densities at ϵ_F in the majority and minority electron spin subband is the inverse of the ratio in nickel (see Sec. 2).

The results of the most complete dHvA measurements in iron at normal pressure were reported in Refs. 21 and 22. Table IV shows a comparison of the measured and calculated dimensions of the sections of the Fermi surface of iron.

We have also attempted to estimate the changes in the

TABLE IV. Comparison of the experimental and theoretical results of the dimensions of the Fermi-surface sections of iron

| Section | Dimension in units of $2\pi/a$ | | Section | Dimension in units of $2\pi/a$ | |
|-----------------------|--------------------------------|---------|-----------------------|--------------------------------|---------|
| | experiment ^[21] | theory* | | Experiment ^[21] | Theory* |
| Minority spin subband | | | Majority spin subband | | |
| $\Gamma-m$ | 0.242 | 0.327 | $\Gamma-a$ | 0.514 | 0.440 |
| $\Gamma-b$ | 0.200 | 0.294 | $\Gamma-c$ | 0.495 | 0.558 |
| $\Gamma-j$ | 0.633 | 0.550 | $H-g$ | 0.110 | 0.082 |
| $\Gamma-i$ | 0.189 | 0.237 | $H-h$ | 0.126 | 0.080 |
| $\Gamma-l$ | 0.545 | 0.581 | $H-i$ | 0.089 | 0.063 |
| $N-n$ | 0.142 | 0.124 | $H-d$ | 0.223 | 0.125 |
| $N-t$ | 0.142 | 0.187 | Lens | 0.05 | 0.05 |
| $H-k$ | 0.355 | 0.325 | radius | | |

*Calculation by the model-Hamiltonian method, present paper.

band structure of iron under pressure, starting from the rigid-band approximation. In particular, the influence of the scale factor, i.e., the increase of the dimensions of the Brillouin zone under pressure, was calculated by us by changing the lattice parameter, but without changing the model-Hamiltonian parameters that describe the potential. We found as a result that the d -bands hardly shift at all, whereas the width W_s of the s band follows the free-electron law, i.e., $d \ln W_s / d \ln V = -0.6 \cong -2/3$.

If it is assumed that the change of the Fermi surface under the influence of the pressure is due only to the transfer of the electrons from the majority spin subband to the minority spin subband then, using relations (5), the experimental BC of the change of the atomic magnetic moment,¹⁶ and the results of our calculation of the state density, we can determine the change of ϵ_F under pressure, in analogy with the procedure used for nickel. As a result we get

$$\delta \epsilon_F^{\uparrow} = \frac{N_{\uparrow}}{N_{\uparrow} + N_{\downarrow}} \delta \Delta = -0.002 \text{ Ry}, \quad \delta \epsilon_F^{\downarrow} = -\frac{N_{\downarrow}}{N_{\uparrow} + N_{\downarrow}} \delta \Delta = 0.005 \text{ Ry}$$

for iron with a lattice constant decreased by 3%, corresponding to a pressure of 173 kbar.

We consider now the section of the lens in the [100] direction, assuming this section to be a circle. At $p=0$ we have $S = 3.8 \times 10^{-2} \text{ \AA}^{-2}$ and at $p=173$ kbar the new position of the Fermi energy yields $S = 7.5 \times 10^{-2} \text{ \AA}^{-2}$. Thus, the BC obtained only as a result of the change of the spontaneous magnetization is equal to -11 . This value is already close to the experimentally observed one. If we add to it the BC of the model metal (molybdenum), which is equal to -3.9 , then we obtain -14.9 , in good agreement with experiment.

Thus, if the BC is represented as a sum of coefficients, due to the scale effect, of the deformations of the potential under pressure and to the spillover of the electrons from one spin-polarization subband to the other, then in the case of iron the main contribution to the summary value, as follows from our estimate, is made precisely by the magnetic spillover. Even this quantity itself is larger by almost one order of magnitude in iron than in nickel, and in addition this term adds up to the BC connected with the deformation potential and with other effects, and is not subtracted as in the case of

nickel. By itself, the large value of B_M is due to the faster change of the position of ϵ_F of iron under pressure than that of nickel, although the changes of the spontaneous magnetizations are close. The indicated faster change is in turn due to the inverse ratio of the state densities in the majority and minority electron spin subbands.

- ¹J. C. Slater, *The Self Consistent Field for Molecules and Solids*, McGraw, 1977.
- ²A. V. Gold, *J. Low Temp. Phys.* **16**, 43 (1974).
- ³I. V. Svechkarev and A. S. Panfilov, *Phys. Stat. Sol. (b)*, **63**, 11 (1974).
- ⁴L. I. Vinokurova, A. G. Gapotchenko, and E. S. Itskevich, *Pis'ma Zh. Eksp. Teor. Fiz.* **26**, 443 (1977) [*JETP Lett.* **26**, 317 (1977)].
- ⁵L. I. Vinokurova, A. G. Gapotchenko, and E. S. Itskevich, *ibid.* **28**, 280 (1978) [**28**, 256 (1978)].
- ⁶E. I. Kondorskii and V. L. Sedov, *Zh. Eksp. Teor. Fiz.* **38**, 773 (1960) [*Sov. Phys. JETP* **11**, 561 (1960)].
- ⁷J. R. Anderson, P. Heiman, J. E. Schirber, and D. R. Stone, *AIP Conf. Proc. No. 29*, Magn. and Magnetic Materials, 1975.
- ⁸V. Heine, *Phys. Rev.* **153**, 673 (1967).
- ⁹J. Hubbard, *J. Phys. C* **2**, 1222 (1969).
- ¹⁰N. I. Kulikov, *Izv. Vyssh. Ucheb. Zav. Chern. Met. No. 7*, 128 (1975).
- ¹¹N. I. Kulikov, *Fiz. Nizk. Temp.* **5**, No. 4, (1979) [*Sov. J. Low Temp. Phys.* **5**, No. 4 (1979)].
- ¹²N. I. Kulikov, A. E. Kadyshovich, Yu. M. Kuz'min, *Izv. Vyssh. Ucheb. Zav. Chern. Met.*, No. 7, 125 (1977).
- ¹³D. C. Gsui, *Phys. Rev.* **164**, 669 (1967).
- ¹⁴S. Wakoh, *J. Phys. Soc. Jpn.* **20**, 1894 (1965).
- ¹⁵E. I. Zornberg, *Phys. Rev.* **B1**, 244 (1970).
- ¹⁶F. Herman and S. Skillman, *Atomic Structure Calculations*, Prentice-Hall, 1963.
- ¹⁷L. F. Mattheiss, *Phys. Rev.* **133**, A1399 (1964).
- ¹⁸S. Wakoh and J. Jamashita, *J. Phys. Soc. Jpn.* **21**, 1712 (1966).
- ¹⁹G. S. Krinchik and E. A. Ganshina, *Phys. Lett.* **23**, 294 (1966).
- ²⁰J. J. Vuillemin and U. J. Bryant, *Phys. Rev. Lett.* **23**, 914 (1969).
- ²¹A. V. Gold, L. Hodges, P. T. Panousis, and D. R. Stone, *Int. J. Magnetism* **2**, 357 (1971).
- ²²D. R. Baraff, *Phys. Rev.* **B8**, 3439 (1973).

Translated by J. G. Adashko